

DETC2007-35418

FRACTIONAL DYNAMICS IN MECHANICAL MANIPULATION

Miguel F. M. Lima*

Dept. of Electrical Engineering
Superior School of Technology
Polytechnic Institute of Viseu
3504-510 Viseu, Portugal
lima@mail.estv.ipv.pt

J.A. Tenreiro Machado

Dept. of Electrical Engineering
Institute of Engineering
Polytechnic Institute of Porto
4200-072 Porto, Portugal
jtm@isep.ipp.pt

Manuel Crisóstomo

Institute of Systems and Robotics
Dept. of Electrical and Computer Engineering
University of Coimbra, Polo II
3030-290 Coimbra, Portugal
mcris@isr.uc.pt

ABSTRACT

This paper analyzes the signals captured during the movement of a mechanical manipulator carrying a liquid container. In order to study the signals an experimental setup is implemented. The system acquires data from the sensors, in real time, and, in a second phase, processes them through an analysis package. The analysis package runs off-line and handles the recorded data. The results show that the Fourier spectrum of several signals presents a fractional behavior. The experimental study provides useful information that can assist in the design of a control system to be used in reducing or eliminating the effect of vibrations.

INTRODUCTION

In practice the robotic manipulators present some degree of unwanted vibrations. In fact, the advent of lightweight arm manipulators, mainly in the aerospace industry, where weight is an important issue, leads to the problem of intense vibrations. On the other hand, robots interacting with the environment often generate impacts that propagate through the mechanical structure and produce also vibrations.

Motivated by the problem of vibrations, this paper studies the robotic signals captured during the motion of a spherical container attached to the manipulator. The container carries a liquid and its acceleration induces motion of the content causing consequently a liquid vibration. The study is done in a fractional calculus (FC) perspective. In order to analyze the phenomena involved an acquisition system was developed. The manipulator motion produces vibrations, either from the structural modes or from the liquid vibration. The instrumentation system acquires signals from multiple sensors

that capture the axis positions, mass accelerations, forces and moments and electrical currents in the motors. Afterwards, the Analysis Package, running off-line, reads the data recorded by the acquisition system and examines them.

Bearing these ideas in mind, this paper is organized as follows. Section 2 addresses the motivation for this work. Section 3 describes the robotic system enhanced with the instrumentation setup. Section 4 presents the experimental results. Finally, section 5 draws the main conclusions and points out future work.

MOTIVATION

Reference [1] mentions several techniques for reducing vibrations and its implementation either at the robot manufacturing stage or at the operational stage. Briefly, the techniques can be enumerate as: (i) conventional compensation, (ii) structural damping or passive vibration absorption, (iii) control based on the direct measurement of the absolute position of the gripper, (iv) control schemes using the direct measurement of the modal response, (v) control driving, actively, energy out of the vibration modes, (vi) use a micromanipulator at the endpoint of the larger manipulator and (vii) adjustment of the manipulator command inputs so that vibrations are reduced or eliminated.

In recent years the study of micro/macro robotic manipulators has been receiving considerable attention. In fact, this approach was employed in manipulators that have been proposed for space applications and nuclear waste cleanup. Several authors have studied this technique [2], namely [3] and [4] that adopted the command filtering approach in order to position the micromanipulator. Also, [4]

* Author of correspondence, Phone: (+351) 232 480 627, Fax: (+351) 232 424 651

and [5] used inertial damping techniques taking advantage of a micro manipulator located at the end of a flexible link. In this perspective, to control the macro/micro system in order to eliminate or reduce the effect of the vibration is fundamental to study the involved variables.

On the other hand, one of the applications where the vibration occurs is in the manipulation of liquids. Here there are two main aspects: the modeling and the control of the liquid dynamics. Several authors addressed the dynamics problem due to liquid slosh loads. There are several mathematical tools to describe the fluids. For example, Navier-Stokes equations [17, 18] can be used to model the liquid dynamics. Concerning the problem of control the liquid vibration, it was first encountered in control of guided missiles in the aerospace industry. In this application it was found that sloshing in the fuel tanks could result in instabilities. Lately, movement of open containers containing fluid, e.g. molten metal and various beverages, has been investigated. The main goal is then to move the container as fast as possible without too much slosh [18, 19].

Bearing these ideas in mind, this article studies the robotic signals, in a fractional system perspective. In fact, the study of fractional order systems has been receiving considerable attention [6, 7] due to the facts that many physical systems are well characterized by fractional models [8]. With the success in the synthesis of real noninteger differentiators, the emergence of new electrical elements [9, 10], and the design of fractional-order controllers [11], fractional algorithms have been applied in a variety of dynamical processes [12]. Therefore, the study presented here can assist in the design of the control system to be used.

EXPERIMENTAL PLATFORM

The developed experimental platform has two main parts: the hardware and the software components. In the following sub-sections these components are briefly described [13].

The hardware components:

The hardware architecture is shown in Figure 1. Essentially it is made up of a robot manipulator, a Personal Computer (PC) and an interface electronic system. The interface box is inserted between the robot arm and the robot controller, in order to acquire the internal robot signals; nevertheless, the interface captures also external signals, such as those arising from accelerometers and force/torque sensors. The modules are made up of electronic cards specifically designed for this work. The function of the modules is to adapt the signals and isolate galvanically the robot's electronic equipment from the rest of the hardware required by the experiments.

The force/torque sensor is the 67M25A model (JR3 Inc), comprising the sensor and a Digital Signal Processing PCI card, and is mounted on the robot's wrist. Two aluminum pancakes were built to mechanically adapt the sensor to the handled object, on one side, and to the robot arm, on the other side. The digital signals from the sensor run through a cable along the length of the arm, and go into a JR3 PCI receiver card inside the PC which processes the data at 8 kHz per axis. The card has built in filtering, but raw force signals were adopted in the following experiments.

Are used two general purpose analog 1-axis piezoelectric accelerometers of type Model FA 208-15, that have a range of ± 5 g, from FGP Instrumentation. The body of the accelerometer sensors is mounted electrically isolated from the manipulator robot in order to prevent ground loops of electrical currents. Actually, without the accelerometers' isolation the signal presents a high level of noise that corrupts the main signal. One accelerometer is attached on the clamped end of the spherical container to measure its oscillations. The second accelerometer is attached on the terminal link of the robot. Both accelerometer signals are processed through an A/D converter.

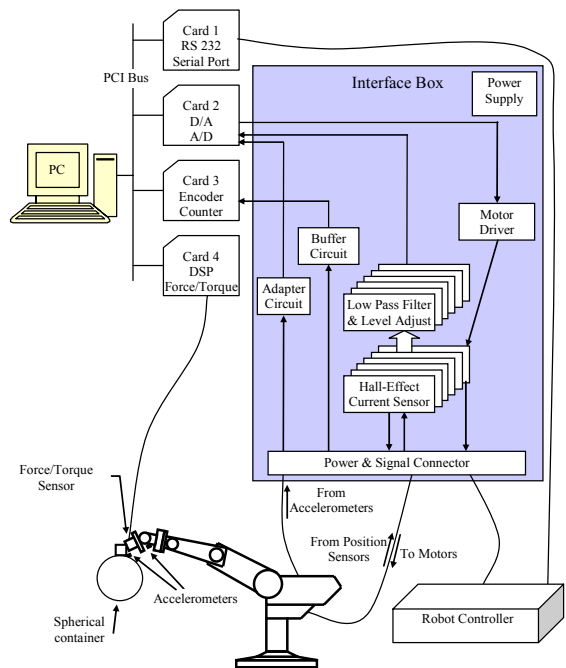


Figure 1. Block diagram of hardware architecture

The robot used is of anthropomorphic type with five degrees of freedom (dof), model Scorbot ERVII from Eshed Robotec. To measure the electrical current supplied to each motor a Hall-effect sensor is inserted to avoid interfere with the robot electronics. A circuit board was developed to handle the signal from the sensor up to the A/D converter. The power supplied to the motors is based on a pulse width modulation (PWM) driver with a frequency of 20 kHz. The motors rotate according with the DC component of electrical current and, in order to measure it, a low-pass filter was implemented for each measurement channel. Thus, a first function of the interface circuit is to filter the high frequency components of the signal and a second function is to isolate galvanically the electrical circuit from the robot electronics.

The robot system has position sensing by means of optical incremental encoders. Those position signals are also captured by the data acquisition system presented here. In order to isolate the robot feedback circuit from the PC card, for each encoder it is inserted a buffer (in the interface box) before connecting the signals to the corresponding high speed counter (in Card 3). This PC card is a high-speed counter/timer, PCI-

6602 model from National Instruments and was programmed to read the signals from the encoders.

The transmitting and receiving of data between the computer and robot is carried out through a serial port RS 232C.

The Software Components:

The Software runs in a Pentium 4, 3.0 GHz PC. The software architecture is shown in Figure 2.

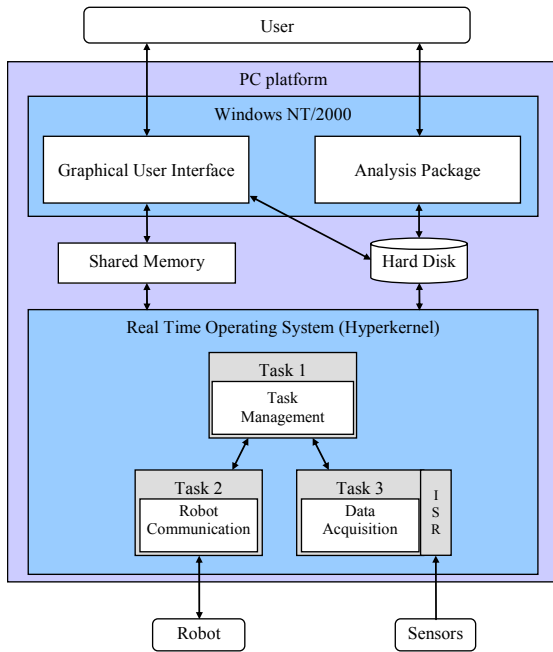


Figure 2. Block diagram of software architecture

The software package developed, from the user’s point of view, consists of two applications. One, the acquisition application, is a program made up of two parts: The Graphical User Interface module and the real time module. The other application is an Analysis Package that analyses the data obtained and recorded by the acquisition application. The real time software, running in the Hyperkernel, was developed in C based on a standard Windows NT/2000 development tool (MS Visual Studio) and the robot controller software was implemented in the ACL proprietary language. The Windows NT/2000 Software is made up of the GUI module of the acquisition system and Analysis Package. The acquisition system software was developed in C++ with MS Visual Studio.

The Analysis Package, running off-line, reads the data recorded by the acquisition system and examines them. The Analysis Package allows several signal processing algorithms such as, Fourier transform (FT), correlation, time synchronization, etc. With this software platform both the Hyperkernel and the Analysis Package tasks can be executed on the same PC.

EXPERIMENTAL RESULTS

In the experiment is adopted a spherical container. Its physical properties are shown in Table 1. To test the behavior of the variables in different situations, the container can

remains empty or its content can be a liquid or a solid. Figure 3 depicts the robot with the container. The robot motion is programmed in a way that the container moves from an initial to a final position following a linear trajectory. The distance between the points is 0.6 m.



Figure 3. Spherical container with liquid

Table 1 – Physical properties of the spherical container

Characteristic	Spherical container
Mass (empty) [kg]	215×10^{-3}
Diameter [m]	203×10^{-3}

During the motion of the manipulator the container is moved by the robot and several signals are recorded with a sampling frequency of $f_s = 500$ Hz. The signals come from different sensors, such as accelerometers, force and torque sensor, position encoders and current sensors. The signals are captured for three different situations: (i) empty container, (ii) container with a solid, and (iii) container with a liquid. The container with the solid or the liquid have an identical mass, namely of 1 kg. In the experiment the used liquid is water. The acceleration of the container induces motion of the liquid. This is referred to as slosh or liquid vibration. The amount of slosh depends on how the container is accelerated, the geometry of the container and the properties of the fluid.

In order to test different acceleration shapes two types of trajectory velocity are used: the trapezoidal and the parabolic profiles (Figure 4). The trapezoidal profile causes the motors to accelerate and decelerate quickly at the start and end of movement, with a constant speed along the path. The parabolic profile causes the motors to accelerate slowly until maximum speed is reached, then decelerate at the same rate.

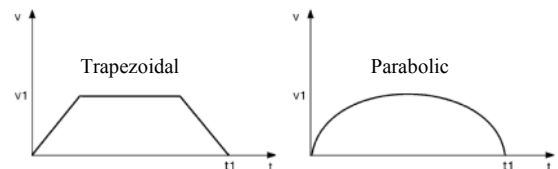


Figure 4. Trajectory velocity profiles

Time Domain:

The time evolution of the variables is shown in the figures 5–14 corresponding to the cases: (i) empty container, (ii) container with a solid, and (iii) container with a liquid.

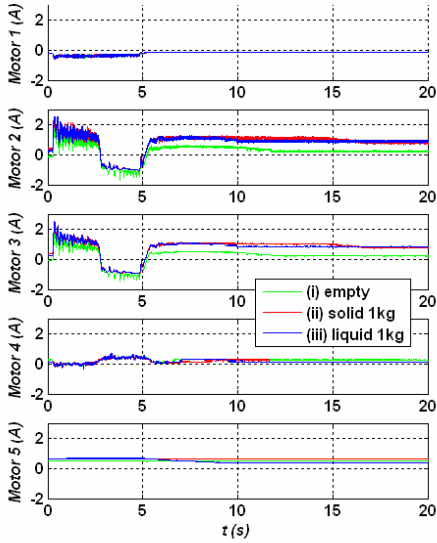


Figure 5. Electrical currents of robot axis motors for the trapezoidal profile

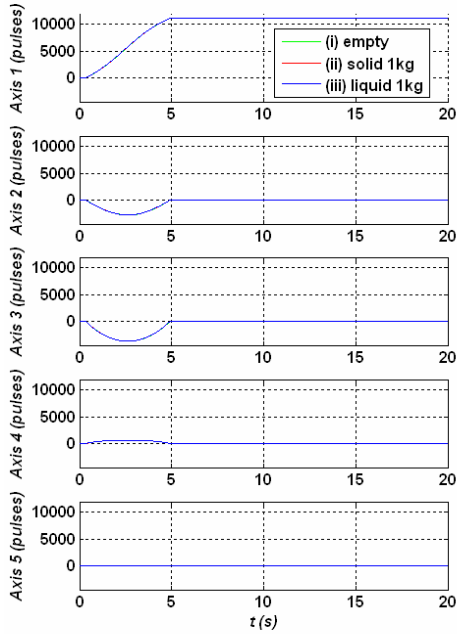


Figure 6. Robot axis positions for the trapezoidal profile

To analyze the vibration effect of the liquid, caused by the container acceleration, the signals are captured during 20 s, although the motion of the container is executed in approximately 5 s.

Figure 5 represents the electrical current of the motors for the trapezoidal profile. As consequence the robot joints rotate as shown in Figure 6. The signals of axis 1 to 4 present a

variation approximately during the first 5 s, that is the time duration of the trajectory. According to the defined trajectory the axis 5 does not rotate.

Figures 7 and 8 show the forces and moments respectively in consequence of the container motion. The effect of the liquid vibration can be observed in the M_y moment component (Figure 8).

Figure 9 shows the accelerations at the clamped end of the

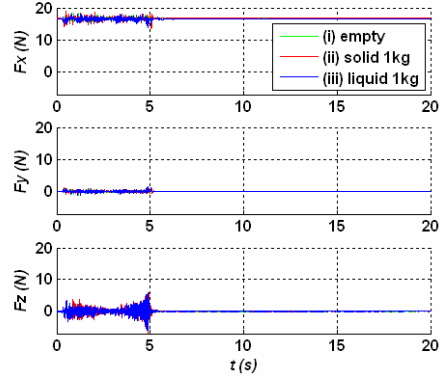


Figure 7. Forces at the gripper sensor for the trapezoidal profile

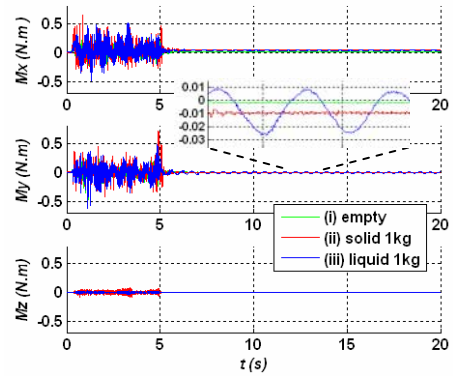


Figure 8. Moments at the gripper sensor for the trapezoidal profile

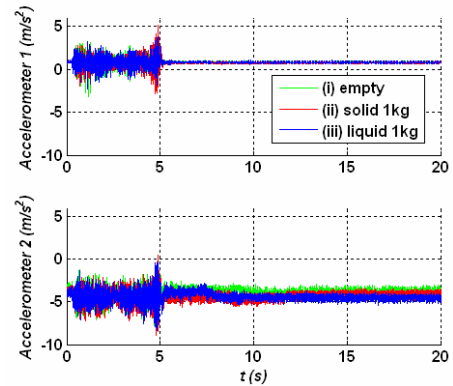


Figure 9. Container and terminal robot link accelerations for the trapezoidal profile

container (accelerometer 1) and at the terminal link of the robot (accelerometer 2). The amplitudes of the accelerometers signals are higher at the end of the container movement.

Figures 10-14 show the time evolution of the variables for the parabolic profile. Comparing the robot axis positions for the two profiles (Figures 6 and 11) it can be seen that the dynamics of the signal positions at the start and end of movement are smoother for the parabolic case. This fact is also reflected in the electrical currents of the robot axis motors (Figures 5 and 10).

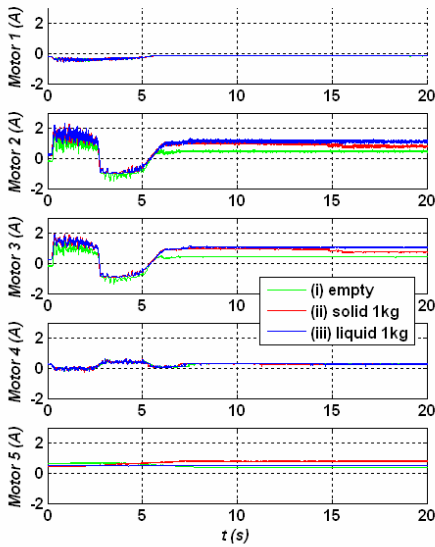


Figure 10. Electrical currents of robot axis motors for the parabolic profile

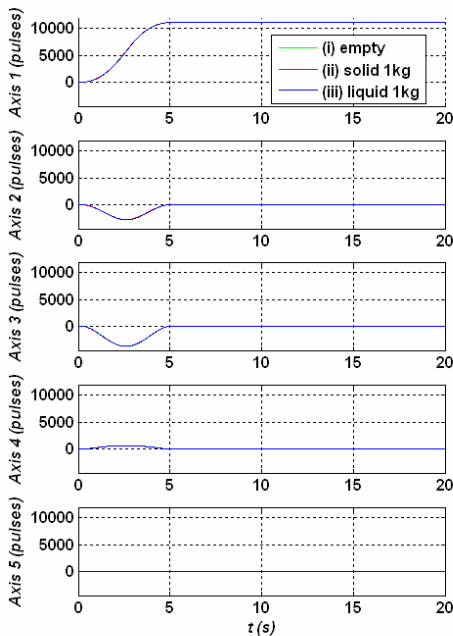


Figure 11. Robot axis positions for the parabolic profile

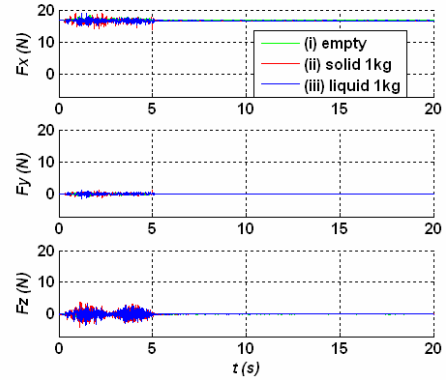


Figure 12. Forces at the gripper sensor for the parabolic profile

The smoother dynamics of the parabolic profile has a consequence of lower forces induced in the container. Therefore, the amplitude of the liquid vibration, caused by the movement of the container, is lower than the acceleration occurring in the trapezoidal case. This fact is reflected in the moments measured at the gripper sensor (see the zoom in Figures 8 and 13). Also, for the trapezoidal profile the accelerations are higher at the end of trajectory, approximately at $t = 5$ s (see Figures 9 and 14).

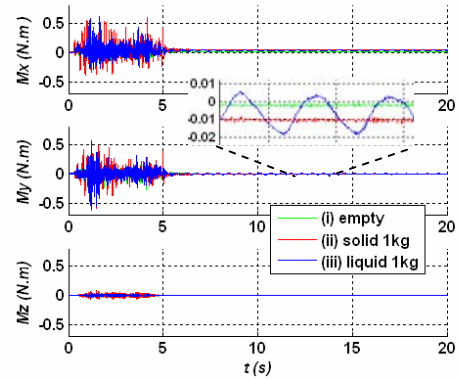


Figure 13. Moments at the gripper sensor for the parabolic profile

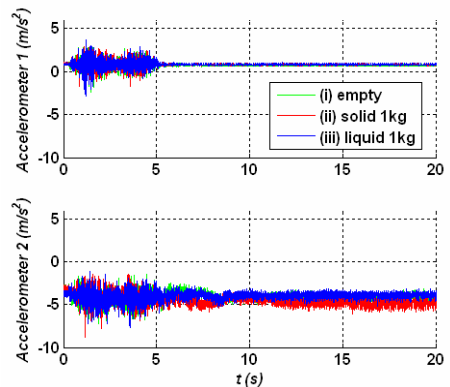


Figure 14. Container and terminal robot link accelerations for the parabolic profile

Frequency Domain:

In order to examine the behavior of the signal FT a trendline is superimposed within the spectrum over, at least, one decade. The trendline is based on a power law approximation [15]:

$$|\mathcal{F}\{f(t)\}| \approx c\omega^m \quad (1)$$

where \mathcal{F} is the Fourier operator, $c \in \mathfrak{R}$ is a constant that depends on the amplitude, ω is the frequency and $m \in \mathfrak{R}$ is the slope.

All the signals of the trajectories referred previously were studied but, due to space limitations, only the most relevant are depicted.

Figure 15 shows the amplitude of the Fast Fourier Transform (FFT) of the axis 1 position signal (case *i*). A trendline was calculated, and superimposed over the signal, with slope $m = -0.99$, that reveals, clearly, the integer order behavior. The position signals present identical behavior, in terms of its spectrum, for the others cases (*ii*) container with a solid and (*iii*) container with a liquid. In fact, as shown before, the position signals maintain the same shape for the three cases (see Figure 6).

Figure 16 shows the amplitude of the FFT of the axis 3 position signal (case *i* and case *iii*). The spectrum is also approximated by trendlines in a frequency range larger than one decade. Here the trendlines present slopes that vary slightly (slope $m = -2.54$ for case *i* and slope $m = -2.50$ for case *iii*). The study of the case *ii*) presents a trendline with a slope of $m = -2.62$. Therefore, the lines present, clearly, fractional order behavior in all cases.

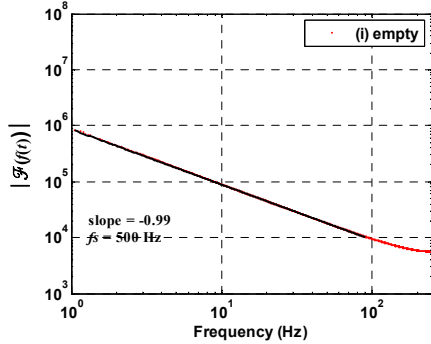


Figure 15. Spectrum of the axis 1 position for the trapezoidal profile

The others position signals (axis 2 and 4) were studied, revealing also a well defined spectrum. Their trend lines present middle slope values that are difficult to classify in terms of its behavior as fractional or integer order. In what concerns to the axis 5 signal position signal, as it maintains the same value during all time acquisition, it consists only in a direct current (DC) component.

Figure 17 shows, as an example, the FFT amplitude of the electrical current for the motor axis 3, that occurs in the case of the trapezoidal profile with container carrying a liquid (case *iii*). A trendline is calculated in a frequency range larger than one decade and superimposed to the signal, with slope

$m = -1.19$. The others current signals were studied, revealing also an identical behavior in terms of its spectrum spread, for the tested conditions (cases *i*, *ii* and *iii*).

According to the robot manufacturer specifications [16] the loop control of the robot has a cycle time of $t_c = 10$ ms. This fact is observed approximately at the fundamental ($f_c = 100$ Hz) and multiple harmonics in all spectra of motor currents (Figure 17).

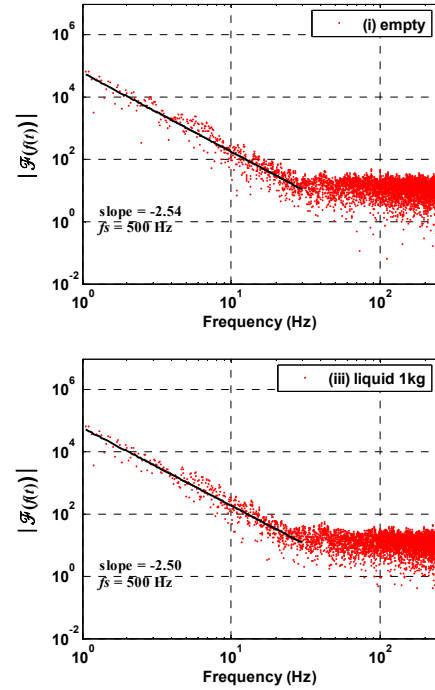


Figure 16. Spectrum of the axis 3 position for the trapezoidal profile

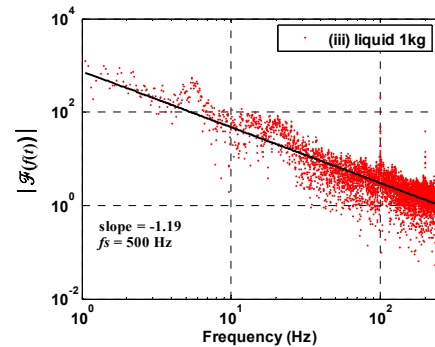


Figure 17. Spectrum of the axis 3 motor current for the trapezoidal profile

Figure 18 shows the FFT amplitude of the F_x force (case *i*) for the trapezoidal profile. A trendline is calculated in a frequency range larger than one decade and superimposed to the signal, with slope $m = -2.52$.

Figure 19 shows the FFT amplitude of the F_y force (cases *i* and *iii*) for the trapezoidal profile. A trendline is calculated in

a frequency range larger than one decade and superimposed to the signal, with slopes $m = -2.49$ and $m = -2.53$, for the cases *i*) and *iii*), respectively. The slope values of the force components presented (Figures 18 and 19) show clearly a fractional order behavior. In general, the forces for the other cases not shown have a spectrum that can be approximated by a trendline in a frequency range greater than one decade. Their trendlines present middle slope values that are difficult to classify in terms of its behavior as fractional or integer order.

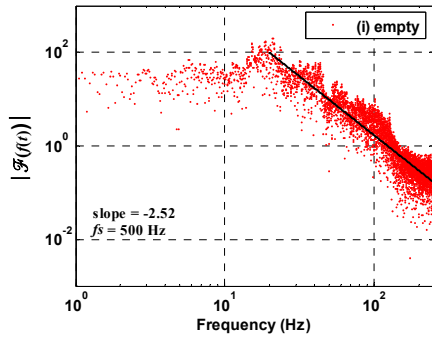


Figure 18. Spectrum of the F_x force for the trapezoidal profile

Figure 20 shows the FFT amplitude of the M_z moment (case *ii*) for the trapezoidal profile. This spectrum is not so well defined in a large frequency range. Moreover, all moments spectra present identical behavior. Therefore, it is difficult to define accurately the behavior of signals in terms of integer or fractional dynamics.

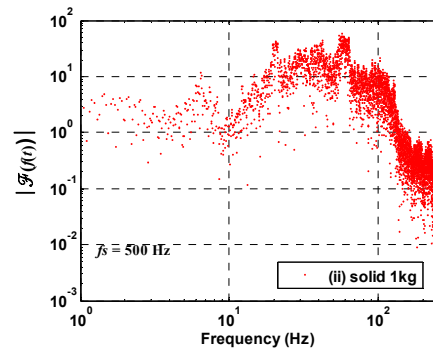


Figure 20. Spectrum of the M_z moment for the trapezoidal profile

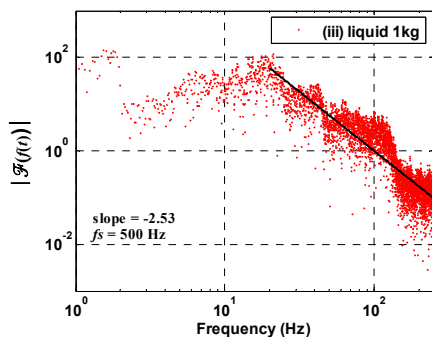
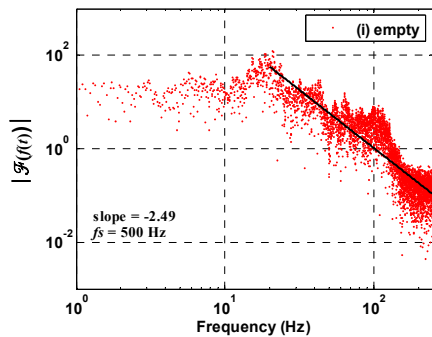


Figure 19. Spectrum of the F_y force for the trapezoidal profile

Finally, Figure 21 depicts the spectrum of the signal captured from the accelerometer 1 located at the container. Like the spectrum from the other accelerometer, this spectrum is spread and complicated. Therefore, is difficult to define accurately the slope of the signal and, consequently, its behavior in terms of integer or fractional dynamics.

The spectra of the captured signals for the trapezoidal profile were studied in terms of their integer *versus* fractional behavior. The spectra signals for the parabolic profile were also analyzed, but due to space limitations are not presented here. Although the signals in time domain for the parabolic profile present a smoother dynamics, comparing with those of the trapezoidal profile, both spectra reveals identical behavior in terms of integer *versus* fractional characteristics.

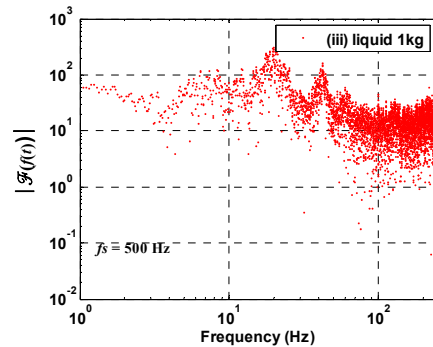


Figure 21. Acceleration spectrum of the container for the trapezoidal profile

CONCLUSIONS

In this paper an experimental study was conducted to investigate several robot signals during the motion of a liquid container. The amount of slosh depends, among other aspects, on how the container is accelerated. In order to test different acceleration shapes two types of trajectory velocity were used: the trapezoidal and the parabolic profiles. Although the signals in time domain present different dynamics for the two profiles, their spectra reveals identical behavior in terms of integer *versus* fractional characteristics. The study was conducted in a fractional system perspective and provides useful information that can assist in the design of a control system to be used in reducing or eliminating the effect of vibrations.

In future work, we plan to pursue several research directions to help us further understand the behavior of the signals. These include the use of a multiwindow algorithm, in order to obtain smoother curves from the scattered spectra. Further investigation of this issue is ongoing.

REFERENCES

- [1] Singer, N. C. and W. P. Seering . Using Acausal Shaping Techniques to Reduce Robot Vibration. Proc. IEEE Int. Conf. on Robotics and Automation. Philadelphia PA., April 25-29, 1988.
- [2] Yoshikawa, T., K. Hosoda, T. Doi and H. Murakami. “Quasi-static Trajectory Tracking Control of Flexible Manipulator by Macro-micro Manipulator System”, Proc. IEEE Int. Conf. on Robotics and Automation, pp. 210-215, 1993.
- [3] Magee, David P. and Wayne J. Book. Filtering Micro-Manipulator Wrist Commands to Prevent Flexible Base Motion. Proc. American Control Conf., Seattle, Washington, June, 1995.
- [4] Cannon, David W., David P. Magee and Wayne J. Book, Jae Y. Lew. Experimental Study on Micro/Macro Manipulator Vibration Control. Proc. IEEE Int. Conf. on Robotics and Automation. Minneapolis, Minnesota, April, 1996.
- [5] Lew, J.Y., Trudnowski, D. J., Evans, M. S., and Bennett, D. W.. Micro-Manipulator Motion Control to Suppress Macro-Manipulator Structural Vibrations. Proc. IEEE Int. Conf. on Robotics and Automation, Vol. 3, pp. 3116-3120, 1995.
- [6] Machado, J. A. Tenreiro. Analysis and Design of Fractional-Order Digital Control Systems, Journal Systems Analysis-Modelling-Simulation, Gordon & Breach Science Publishers, vol. 27, pp. 107-122, 1997.
- [7] Machado, J. A. Tenreiro. A Probabilistic Interpretation of the Fractional-Order Differentiation, Journal of Fractional Calculus & Applied Analysis, vol. 6, No 1, pp. 73-80, 2003.
- [8] Podlubny, I.. Geometrical and physical interpretation of fractional integration and fractional differentiation. Journal of Fractional Calculus & Applied Analysis, vol. 5, No 4, pp. 357-366, 2002.
- [9] Bohannan, Gary W.. Interpretation of Complex Permittivity in Pure and Mixed Crystals, www.gl.ciw.edu/~cohen/meetings/ferro2000/proceedings/bohannan.pdf, 2000.
- [10] Bohannan, Gary W.. Analog Realization of a Fractional Control Element -Revisited mechatronics.ece.usu.edu/foc/cdc02tw/cdrom/additional/FOC_Proposal_Bohannan.pdf, 2002.
- [11] Barbosa, Ramiro S., J. A. Tenreiro Machado and Isabel M Ferreira. Tuning of PID Controllers Based on Bode’s Ideal Transfer Function, Nonlinear Dynamics 38: pp. 305–321, Kluwer Academic Publishers, 2004.
- [12] Oustaloup, Alain, Xavier Moreau and Michel Nouillant. From fractal robustness to non integer approach in vibration insulation: the CRONE suspension, Proceedings of the 36th Conference on Decision & Control, San Diego, California, USA, December, 1997.
- [13] Lima, Miguel F. M., J.A. Tenreiro Machado, and Manuel Crisóstomo. Experimental Set-Up for Vibration and Impact Analysis in Robotics, WSEAS Trans. on Systems, Issue 5, vol. 4, May, pp. 569-576, 2005.
- [14] Lima, Miguel F. M., J.A. Tenreiro Machado, and Manuel Crisóstomo. Fractional Order Fourier Spectra In Robotic Manipulators With Vibrations, Second IFAC Workshop on Fractional Differentiation and its Applications, Porto, Portugal. 2006.
- [15] Lima, Miguel F. M., J.A. Tenreiro Machado, and Manuel Crisóstomo. Windowed Fourier transform of experimental robotic signals with fractional behavior. In Proc. IEEE Int. Conf. on Computational Cybernetics, pages 21-26, Tallin, Estonia, August, 2006.
- [16] Scorbot ER VII, User’s Manual, Eshed Robotec, 1996.
- [17] Rumold, W.. Modeling and Simulation of Vehicles Carrying Liquid Cargo, Multibody Systems Dynamics 5: 351-374, 2001, Kluwer Academic Publishers.
- [18] Grundelius, M.. Methods for Control of Liquid Slosh. PhD thesis, Lund Institute of Technology, Sweden, October 2001.
- [19] Feddema, J.T., C.R. Dohrmann, G.G. Parker, R.D. Robinett, V.J. Romero, and D.J. Schmitt. Control for slosh-free motion of an open container. IEEE Control Systems, 17(1):29–36, February 1997.